Behavior of Glazed Facades under Explosions Action
Development of a protective solution

Rui Jorge Lourenço Rita
ruijlr@gmail.com
IST, Instituto Superior Técnico, Portugal
AM, Academia Militar, Portugal

Abstract

Terrorism in today's societies can refer to its various forms. However, the form that interests this work is the use of explosive devices. These devices, improvised or not, constitute a global threat to human beings, beings entitled to security and protection.

Military and Civil Engineering have made efforts and done research in order to promote the design of critical infrastructures subjected to the dynamic actions of explosions. They have also invested in the study, development and implementation of protection systems capable of mitigating the impacts of explosions, both on the structure itself and on its occupants.

Glass is a transparent and sustainable material, widely used in modern glass facade systems, for example in public and military buildings, with strategic nature, such as government buildings, barracks, airports, bus terminals, hospitals and universities.

When an explosion hits a building, the facades are one of the most vulnerable elements.

The protection system studied consists of an energy dissipator inserted in a pinned connection system. The dissipator is made of metamaterial and has hexagonal alveolar geometry, capable of plastic deformation and containing, at a local level, the destructive effects that would pass to the building's main structure, through the glass facade. The facade also has the role of protecting from the outside those who are inside the protected space and in order to do it, it's extremely important that the glass facades are composed of laminated glass.

Keywords: Explosive devices; Protection systems; Glazing facades; Connection systems; Metamaterials; Laminated glass.

I. Introduction

The safety of an individual is a basic human right and the protection of individuals is a fundamental obligation of the Government. Therefore, states have an obligation to guarantee human rights by taking positive steps to protect against the threat of terrorist acts and to bring the perpetrators of such acts to justice [1].

According to the Global Terrorism Database (GTD), a terrorist attack is defined as the threat or even use of illegal force and violence by a non-state in order to achieve a political, religious, social or economic objective through fear, coercion or intimidation [2].

Traditionally, terrorists have chosen buildings as their preferred target for malicious attacks. Buildings are roughly constructed according to codes, and in most cases the prevention and minimization of the impact of chemical, biological, radiological and nuclear (CBRN) and explosive ordnance attacks is missing in the design. [3].

Using glass as a construction material takes us a long way back in time, but it is in the last decades that new functions and challenges for its use are known. Glass presents a range of mechanical characteristics that looking from the structural point of view represent limitations that must be treated with care, being that its fragility will be the core [4], [5].

When the pressure of an explosion fractures a glass, the shrapnel that falls and is projected, represents a great risk for those who are close by. The use of explosion-proof or explosion-protected glazing on buildings likely to be subjected to such a load may greatly reduce, if not eliminate, the associated risks. Taking these aspects into account, in the case of glazing, constitutes a significant reduction in damage inside buildings and the "cleanliness" that an explosion entails [6].

The main objective of this work is the study of heat sinks with different (but similar) mechanical characteristics, inserted in the same fixing structure of the glass façade and subject to the same explosion action. The methodology used in the modeling was to first design a .iges file with the geometry of the structure drawn to the midline; import this file into the modelling software and create a reference model that did not contain the developed protective solution, working as a zero test. Then a model was developed with the dissipator already integrated and that was viable, so models were runned in which the dissipators had different characteristics.

II. Explosion Action

Dynamic loads encompass situations that static ones do not contemplate. They can have several origins, such as human activity, wind, earthquakes, impacts and, of course, explosions. An explosion is defined as a rapid release of energy on a large scale [7].

Explosions can be divided into two main groups according to the confinement of the explosive charge: confined and unconfined.

Non-contained, non-contact or external explosions, as mentioned, can be divided into 3 basic types, which depend on the relative position of the source of the explosion and the structure to be protected. These three types of explosion correspond to: Perfect air explosion; near surface explosion [8], [9]; surface explosion. In the case of confined or interior explosions, they will be amplified by the phenomenon of reflection within the building itself. There are 3 types of confined explosions, according to the size of the ventilation concerned: Fully ventilated explosion; Partially confined/ventilated explosion; Fully confined explosion. The definition of the shockwave parameters used most often is based on Kinney and Graham's expressions [10] and on the proposals of Kingery and Bulmash, in 1984 [11].

On **Ilustration 1** is illustrated the idealized pressure variation profile with the time of explosion, characterizing the explosion itself.

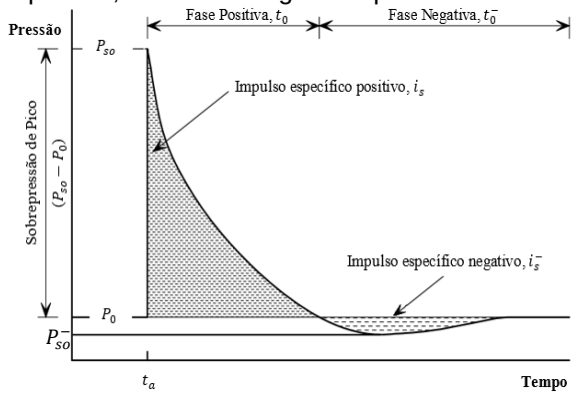

Ilustration 1 – Idealized pressure profile (adapted from [9]).

The following modified Friendlander equation (2.1) proposes and is often used to describe the rate of decrease in positive phase pressure values:

$$P_s(t) = P_{so} \times \left(1 - \frac{t}{t_0}\right) e^{-b\frac{t}{t_0}} \qquad (2.1)$$

where, P_{so} [kPa] represents the peak incident overpressure, t_0 [ms] is the duration of the positive phase, b is the decay coefficient of the curve and t [ms] corresponds to the period between the arrival instant (t_a) and the instant in study [11].

Although there is bibliography [12] which analyzes in detail possible values for the decay coefficient of the curve (*b*), in the design of structures it is usual to take conservatively a linear rate of decrease of pressures [13], [14], [15], [16].

It should be noted that this alternative, which is really conservative, is expressed in the equation (2.2).

$$P_s(t) = P_{so} \times \left(1 - \frac{t}{t_0}\right) \qquad (2.2)$$

When the shock wave reaches an obstruction, it reflects in amplitudes of a higher value than the initial one. The reflection is a function of the force of the explosion and the incidence angle of the shock wave front [14].

2.1. TNT Equivalency

The need arises to compare the effects of explosions originated by different explosives, which can be done by the TNT Equivalency method.

The equivalence in TNT, from the numerical point of view, can be given by the following equation (2.3), present in UFC 3-340-02 [8]:

$$W_{TNTe} = \frac{H_{EXP}^d}{H_{TNT}^d} \times W_{EXP} \qquad (2.3)$$

where, W_{TNTe} represents the equivalent mass of TNT, W_{EXP} the mass of the explosive in question, H_{EXP}^d the heat of explosion for the explosive in question and H_{TNT}^d the heat of explosion of TNT.

2.2. Scaled distance

This parameter is a scalar and means that when two explosive charges of different size but the same geometry and type of explosive are detonated in the same environment, the shock waves generated are equal if they have equal scaled distance. The following equation (2.4) defines the relation, formula of Hopkinson (1915) and Cranz (1926):

$$Z = \frac{R}{\sqrt[3]{W}} \qquad (2.4)$$

where Z is the scaled distance $\left[m/kg^{1/3}\right]$, R is the distance between the target surface and the epicentre of the explosive charge $[m]$ and W the mass of the explosive charge $[kg]$ [8], [17]

2.3. Peak overpressure

One of the formulas that exist to characterize the peak overpressure [MPa], is Kinney and Graham equation [10] (2.5).

$$P_{so}[MPa] = \frac{808 \times \left[1 + \left(\frac{Z}{4,5}\right)^2\right] \times P_0}{\left[1 + \left(\frac{Z}{0,048}\right)^2\right]^{1/2} \times \left[1 + \left(\frac{Z}{0,32}\right)^2\right]^{1/2} \times \left[1 + \left(\frac{Z}{1,35}\right)^2\right]^{1/2}} \qquad (2.5)$$

2.4. Incident specific impulse

This same shock wave characterization parameter translates into the area below (i_s) and above (i_s^-) the curve (**Ilustration 1**). The following equations translate the specific positive (2.6) and negative (2.7) impulses:

$$i_s = \int_{t_a}^{t_a+t_0} P_s(t)dt = \frac{P_{so} \times t_0}{b} \times \left[1 - \left(\frac{1 - e^{-b}}{b}\right)\right] \qquad (2.6)$$

$$i_s^- = \int_{t_a+t_0}^{t_a+t_0+t_0^-} P_s(t)dt = -\frac{P_{so} \times t_0}{b^2} \times e^{-b} \qquad (2.7)$$

Kinney and Graham [10], have also developed an empirical expression that allows,

only with the scaled distance variable, the calculation of the specific impulse in positive phase:

$$i_s[MPa \cdot ms] = \frac{0{,}0067 \times \sqrt{1 + \left(\frac{Z}{0{,}23}\right)^4}}{Z^2 \times \sqrt[3]{1 + \left(\frac{Z}{1{,}55}\right)^3}} \quad (2.8)$$

2.5. Dynamic peak overpressure

In UFC 3-340-02 [8] are present the results for Newmark's (2.9) (developed for low pressures and atmospheric conditions at sea level) and Rankine-Hugoniot (2.10) equations [8], [18]:

$$q_s = 0{,}022 \times (P_{so})^2 \quad (2.9)$$

$$q_s = \frac{5}{2}\frac{(P_{so})^2}{(7P_0 + P_{so})} \quad (2.10)$$

2.6. Duration of the positive phase

Kinney e Graham [10], present the equation (2.11) that makes it possible to calculate the duration of the positive phase (t_0):

$$t_0[ms] = \frac{980 \times \left[1 + \left(\frac{Z}{0{,}54}\right)^{10}\right] \times \sqrt[3]{W}}{\left[1 + \left(\frac{Z}{0{,}02}\right)^3\right] \times \left[1 + \left(\frac{Z}{0{,}74}\right)^6\right] \times \left[1 + \left(\frac{Z}{6{,}9}\right)^2\right]^{1/2}} \quad (2.11)$$

2.7. Reflection of the shock wave

The shock wave, which intersects a solid surface, will be subject, in its course, to phenomena of amplification and reflection. There are three types of reflection, depending on the angle of incidence, normal, oblique and the resonant. The most severe case, as far as the loading of the structure subject to the explosion is concerned, is the normal reflection that happens when the surface is perpendicular to the direction of propagation of the wave.

Rankine and Hugoniot (2.12), propose the method that admits that air has the behavior of a perfect gas and considers the blowing effect of dynamic pressures originated by the flow of gases generated by the passage of the shock wave [19].

$$P_r[MPa] = 2 \cdot P_{so} \times \left(\frac{7 \cdot P_0 + 4 \cdot P_{so}}{7 \cdot P_0 + P_{so}}\right) \quad (2.12)$$

In structure design, the peak reflected overpressure can be calculated by a triangular approximation of one impulse, where the maximum value is P_r and the duration time is t_0. Therefore the relative impulse, i_r, is calculated according to equation (2.13):

$$i_r = \frac{1}{2} \cdot P_r \cdot t_0 \quad (2.13)$$

It is also important to emphasize that Needham [19] suggests the use of equation 2.14 as opposed to the previous equation (2.13), since it states that it overestimates the value of the reflected impulse:

$$\frac{i_r}{i_s} \approx \frac{P_r}{P_{so}} \quad (2.14)$$

However, there is an expression (2.15) that uses the reflection coefficient, which has adimensional value, thus enabling the analysis of oblique reflection. This is the most usual and comprehensive expression [9], [11]:

$$P_r = P_{so} \times C_r \quad (2.15)$$

2.8. Response to explosion action

In cases where the reflected shock wave intersects the incident, it results in only one wave, amplified, formed in the plane of reflection. The resulting wave is called *Mach stem* or resonant wave. The resonant wave is based on the fact that the incident wave cannot be surpassed by the reflected wave; it is a plane wave and its height increases along the propagation [17].

When the shock wave affects the face of a structure, complex phenomena are created The structure is subject to an action that will equal the pressure reflected by it. Thus the analysis of the response of the structure as a whole is characterized, not by the action imposed on the global structure, but by the rupture of elements considered critical [10], [17].

The frontal surface of the structure is therefore the most conditioning because it is subject to peak, dynamic and reflected pressures. The total load force of an explosion is given by the equation (2.16), where $F_{impulsive}$ (2.17) is the parcel referring to the shock wave, and $F_{dynamic}$ (2.18) is the load that results from the flow of air after the shock wave (dynamic pressure). The unknown A_{proj} corresponds to the area of the structure in design perpendicular to the shock wave and C_D represents the drag coefficient. This coefficient for the front surface of a building has a value equal to one [9].

$$F(t) = F_{impulsive}(t) + F_{dyanmic}(t) \quad (2.16)$$

$$F_{impulsive} = P_r \cdot A_{proj} \quad (2.17)$$

$$F_{dynamic} = q_s \cdot C_D \cdot A_{proj} \quad (2.18)$$

2.8.1. Response regimes

The charge of an explosion imposed on a structure transmits energy, making it behave in a dynamic way. How a structure or structural element responds to an explosion charge is entirely linked to the relationship between its natural period of vibration (T) and the duration of the positive phase of the wave (t_0) (2.19) [5]:

$$\frac{t_o}{T} \quad (2.19)$$

Between the impulsive and quasi-static regime, there is a more complex one, usually called the dynamic regime. In this regime, the duration of the charge is identical to the period of vibration of the structure and the time it takes to respond, thus amplifying the response. This response is therefore given at the same time as the loading [9].

For a given structure and type of load (e.g. pressure), it can be graphed as an iso-response curve, also called a pressure-impulse (P-I) diagram. Its analysis suggests that as the request duration increases, the response becomes changeable due to the maximum value of pressure and not impulse [11].

III. Technology of glazed facades

3.1. Glazing

Glass is a material that results from a rapid cooling of molten material, which will reach a certain rigidity in its hardening, but without crystallization occurring. In general, and according to the **Ilustration 2**, silica represents more than 70% of the total original matter, has melter portion, a stabilizer, and other oxides [20].

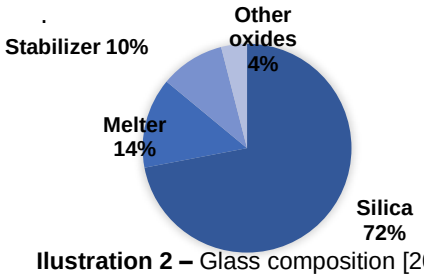

Ilustration 2 – Glass composition [20].

There are 4 types of glass according to its manufacturing method: float glass (common glass of slow cooling); annealed glass (reheated float glass); tempered glass (it suffers the hardening process that installs superficial stress (pre-stressing)); and thermally thoughned glass (hardening not as fast as in the tempered glass).

Regarding its use in facades, the glass can be: monolithic (a glass sheet); laminated (2 or more sheets separated by PVB or other polymer films); and insulating (glass sheets with a space between them, which can be filled or not). Then, in **Table 1**, we have the most relevant properties of the glass for this work (mechanical properties of tempered glass):

Property	Values
Density (kg/m3)	2500
Young Modulus *E* (GPa)	70 – 75
Distortion Modulus *G* (GPa)	26 – 33
Poisson's coefficient ν	0,20 – 0,25
Compression stress (MPa)	400 – 1000
Pull stress (MPa)	250
Bending stress (MPa)	120

Table 1 – Mechanical properties of tempered glass (adapted from [20]).

The following are the properties of the intermediate layer that matters for this work – the PVB (**Table 2**):

Property	Values
Young Modulus (E)	985 MPa
Pull stress (f_t)	28 MPa
Failure strain (ε_t)	≥ 300 %
Density (ρ)	1,07 g.cm^{-3}
Poisson's coefficient (ν)	0,49

Table 2 – PVB properties (adapted from [5], [21], [22])

3.2. Connection systems

The main objective of a glass fixing system is to mitigate direct contact between the glass and the metal components that are normally used in the support. Nowadays it is perfectly possible to build glass facades without the use of traditional window frames, thus making it possible to reduce the visual obstruction by reducing the size of the fixing/connection systems. However, this decrease increases the stresses installed in the glazing [5], [20]. The following is a summary diagram of the connection systems and their types (**Ilustration 3**):

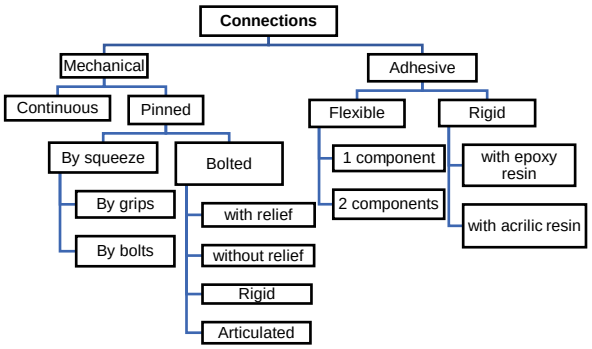

Ilustration 3 – Connection systems summary.

3.3. Suporting structure (study case)

The total support structure is therefore supporting 2 panels of laminated tempered glass 2 meters wide and 3 meters high. It can be separated into two structures, the main supporting structure and the secondary supporting structure. The main supporting structure corresponds to 3 IPE200 profile columns in S275 steel. Each IPE200 has, fixed to itself, 3 fixing systems (secondary support structure): one at the top, one at half height and one at the base. In this structure (S275) only the perpendicular plates have a different steel - S460. A diagram of the secondary support structure is shown at the bottom (**Ilustration 3**):

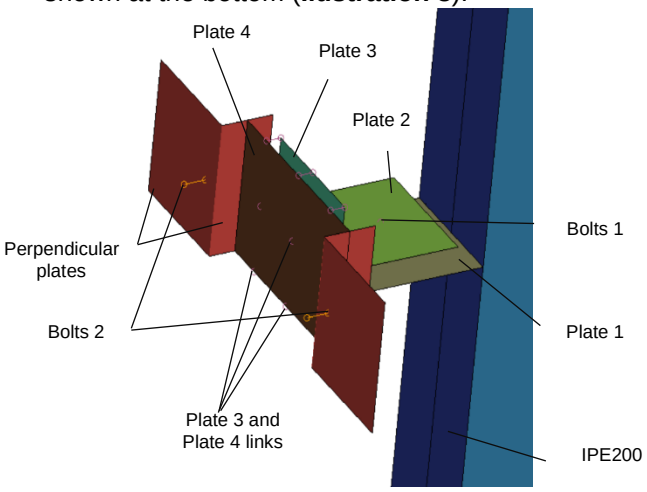

Ilustration 4 – Secondary support structure.

3.4. Energy-absorbing polymeric devices

The energy absorption devices that become important to study are the polymeric constitution devices, due to the fact that the protection solution that is intended to develop, in this dissertation, involves an energy dissipator in Polyethylene terephthalate glycol (PETg). Low density materials, capable of minimizing the damage caused by an impact load, are of extreme importance for the protection of structures that require it. While conventional materials have properties that depend on their composition and stability of chemical bonds, metamaterials have properties that depend on the physical geometry of the structures that constitute them. Mechanical metamaterials consist of conventional materials. However, their geometry makes them have more interesting and superior physical properties than the conventional constituent material [23].

IV. Structural analysis of facades subject to an explosion

Laminated glass panes are, in large scale, the best choice in the design of glass subject to explosions. The shards of laminated glass remain adherent to the intermediate layer in the post-break, thus reducing the threat of projection to the surrounding area. If the interlayer is correctly designed then it does not break and works as a boundary between the shock wave and the interior of the building. Analytical and numerical methods are necessary in order to determine the structural behavior of laminated glass under explosions, since there is great complexity regarding the load and structural response. Three possible methods to be used in the structural analysis of glass elements are presented next.

4.1. Simple-Degree-of-Freedom System

Structural elements subject to dynamic actions can be modeled in a simplified way using a system of a degree of freedom – SDOF – consisting of a mass, a spring and a buffer [18], [24]. This method gives approximate results for the maximum deformations installed, without being able to determine within a time interval. For accelerations, this method reveals worse approximations, as it is too simple in the case of a complex structure, as is the case of this work [18].

4.2. Behaviour of the glass plate

The behavior of the glass plate can be approximated using Kirchhoff's slab theory. According to this theory, a slab is a structural element of thickness with a much smaller dimension than the other dimensions subject to actions outside its plane, which produce a curvature of the surface of the glass slab [24].

Slab theory provides adequate results when small deformations occur. However, glass panels suffer great deformations under explosion loads (the membrane forces are also activated). These membrane efforts also have an influence on the degree of curvature when the deformation exceeds the panel thickness. In general, the basic equations of slab theory, used in thin panels with large deformations, are extremely difficult to solve because of the geometric non-linearity associated with the problem in question. There are only a few analytical solutions specific to basic problems [15]. Thus, the solution of these problems is usually obtained by iterative numerical methods based on the Finite Element Method.

4.3. Finite Elements Method (FEM)

The Finite Element Method (FEM) is the most appropriate numerical method to solve complex problems (which analytical methods are unable to solve or very difficult to solve) associated with: material properties, loads or complicated geometry. The FEM models require a discretization where smaller elements are created linked by us. The right and certain equations are solved for each connecting node, until a stable solution emerges [24].

Software such as ANSYS®, ABAQUS®, SAP2000®, Robot Structural Analysis® and LS-Dyna®, are some of the structural analysis programs by FEM currently marketed. In these programs the user/engineer must fully define the problem, i.e. design or import the geometry, establish the appropriate material models and breaking criteria, create the finite element mesh and apply the loading and boundary conditions. FEM programs are widely used by researchers who use experimental results to validate their computational models. On the other hand, FEM is considered very expensive in terms of time, for those who dimension on a day-to-day basis, i.e., FEM serves more for complex dimensioning problems [24]. In the following section a brief reference will be made to the software used to model the case study of this dissertation.

4.4. LS-Dyna Software

LS-Dyna is an advanced general purpose simulation software developed by Livermore Software Technology Corporation (LSTC). It is a structural analysis software that uses finite elements to simulate complex real life problems and is widely used in the military, aerospace, automotive, among others. The program solves problems that include geometric or contact nonlinearities, complex material constituent relationships or large deformations. The models that involve explicit calculation have, in most cases, very short time intervals, as is the case that this dissertation intends to study. In the explicit calculation of finite elements, the equation of motion is solved by increments, and the stiffness

matrix is updated at the end of each displacement and load increment, based on the change in material definition and geometry. Regarding the time increment, it is automatically determined by LS-Dyna, based on the algorithm proposed by Newmark, which was developed studying the speed of sound in a certain material. Generally, the experimental results obtained by the user are compared with the results obtained by the LS-Dyna simulations [25], [26].

V. Study case – Analysis of structural behavior

5.1. Study case description

The IPE200 profile will then be 3 meters high and will be oriented so that it resists horizontal loads with its axis of greater inertia. It is embedded at the base and has a fixed support at the top, being therefore a hyperstatic structure of grade 2.

Each fixation system is composed of 4 plates, 2 quinad plates, 3 screws and several welding beads.

The geometry of the fixation has undergone major changes over the months of work and the final geometry was inspired by photographs of glazed facades of the Madrid airport. In **Ilustrations 5 and 6**, it is possible to visualize the similarities with the fixation system adopted in this work.

Ilustrations 5 and 6 – Inspiration of the connection system used (Madrid Airport).

As it was mentioned the constitution of the support structure, now reference will be made to the glass used in modeling and its characteristics.

As far as laminated glass panels are concerned, it was first decided to use laminated glass because, when talking about an explosion action, it is necessary to have safety glass that retains as much as possible the fragments of glass that can damage those in the surrounding area. Secondly, tempered laminated glass by its evident properties and superior advantages. However, it is necessary to design the glass for the action of explosion, and this was done according to the European pre-norm 16612 (prEN16612).

Regarding the dimensioning of the resistant capacity of the tempered glass, it can be calculated using the following expression (5.1), whatever the composition of the glass is:

$$f_{g;d} = \frac{k_{mod} k_{sp} f_{g;k}}{\gamma_{M;A}} + \frac{k_v (f_{b;k} - f_{g;k})}{\gamma_{M;v}} \qquad (5.1)$$

where $f_{g;k}$ is the characteristic value of the bending stress; $\gamma_{M;A}$ is the partial coefficient of safety for the annealed glass; k_{sp} is the coefficient of behaviour of the glass surface; k_{mod} is the coefficient of load duration; $\gamma_{M;v}$ is the partial coefficient of safety of tempered glass; $f_{b;k}$ is the characteristic value of the bending stress of tempered glass; k_v is the hardening factor of tempered glass.

The value of k_{mod} can be calculated by the following formula (5.2), as it can be used for loading durations below 20 milliseconds:

$$k_{mod} = 0{,}663 t^{-\frac{1}{16}} \qquad (5.2)$$

Conservatively, for a duration of 15 ms corresponding to the action of the explosion, a k_{mod} of 1.438 is obtained by the previous expression.

For the coefficient of behaviour of the glass surface k_{sp}, is taken the value of 1,0 for laminated glass, as it is in prEN. Is considered 45 N/mm^2 (MPa) as the characteristic value of the bending tension, $f_{g;k}$, as stated in the prEN. The value of the partial coefficient of safety of the material for annealed glass ($\gamma_{M;A}$) is then 1.8 and for tempered glass ($\gamma_{M;v}$) it is 1.2, for the ELU (the only values supplied in the prENorm). For the value of the reinforcement factor of the prestressed glass (k_v) 1.0 will be used which corresponds to a horizontal hardening relative to the manufacturing process. Regarding the value of the bending characteristic stress for tempered glass, the value of 120 N/mm^2 corresponding to safety glass thermally hardened or heat soaked.

Finally, they have a necessary resistant stress of:

$$f_{g;d} = \frac{1{,}438 \,.1{,}0 \,.45}{1{,}8} + \frac{1{,}0.(120-45)}{1{,}2} = 98{,}45\ MPa$$

According to the standard, using this value and a set of expressions, it would be possible to take the value of the thickness of each of two sheets of a laminated tempered glass panel, as desired. However, the values reached were very low. So, and in a somewhat empirical way by experience of the orientation of the present dissertation, it was decided in some meetings, to use two 8 mm thick tempered glass sheets connected by a PVB film.

Regarding the thickness of the PVB film to be used, it can infer it by the dimensions of the laminated glass of the study case.

Now, knowing that we have two sheets of 8 mm, we will have 16 mm of ordinary thickness, then last line of the table. As each glass panel of the case study is 2 meters wide (which is the smallest gap), then we will need a PVB film with 1.52 mm of thickness.

Therefore, as said, we will need a laminated glass 88.1, two sheets of 8 mm plus a

PVB film of 1.52 mm, which makes a total thickness of 17.52 mm necessary. This thickness is already acceptable for a facade that is being dimensioned for the action of an explosion.

Regarding the explosive charge, there is 10 kg of TNT placed 5 meters away from the outer face of the facade and 1.5 meters high from the ground, which corresponds to half the height of the facade. It was considered that the most serious case for the structure would be to align the load with the profile, which symbolizes the main structure, and the height of the supports of half of the panels, to enhance the response of the support that is in that location and halfway from the profile.

5.2. Modelling

The whole model has its geometry drawn to the middle line so that it would be possible to work only with 2D elements, like Shell or Beam, in order to make the three-dimensional model lighter and not take as long to run as a three-dimensional model consisting of 3D elements. The geometry of the model was made and imported, almost in its entirety, from the AutoCAD software so that it was only necessary to characterize the elements, boundary conditions and actions in LS-Dyna, considered a complex program. After having the geometry inserted in the software, it was proceeded, in order: - The creation of entities (the PART keywords) for each element with different characteristics;

- Creation of plate and beam elements (keywords ELEMENT_SHELL and ELEMENT_BEAM) from the imported lines of the AutoCAD drawing program;
- Creation of the desired section (thickness) for each of the Shell and Beam elements, through the keywords SECTION_SHELL and SECTION_BEAM;
- Choose, from the range of options of LS-Dyna, the materials to be used and assignment of the characteristics requested by the program, in the keyword MAT;
- Assignment of the type of element, section and material to each entity in the existing keyword PART;
- Choice of a relatively thin mesh for each entity, now with defined characteristics and properties;
- Choice of the support conditions and boundary of the structure modeled, taking into account the simplification of geometry, in keyword BOUNDARY_SPC_SET;
- Definition of the contacts (keyword CONTACT) between the various elements that are connected to each other and that may touch each other with the development of the loading action;
- Definition of the parameters of the explosion action and the area of incidence of the explosion, in the keywords LOAD_BLAST_ENHANCED and LOAD_BLAST_SEGMENT_SET, respectively;
- Choice of the parameters of the development time of the explosion action, in the keyword CONTROL;
- Selection of the files that the program creates with results of the action, in the keyword DATABASE.

5.3. Results for an explosion

One of the main indicators of the load passing to the structure is the maximum axial and shear force verified in *Bolts 1*, along the facade. In the next **Ilustration 7, Ilustration 8** and **Ilustration 9**, are graphs with these results are presented for a 70 ms analysis.

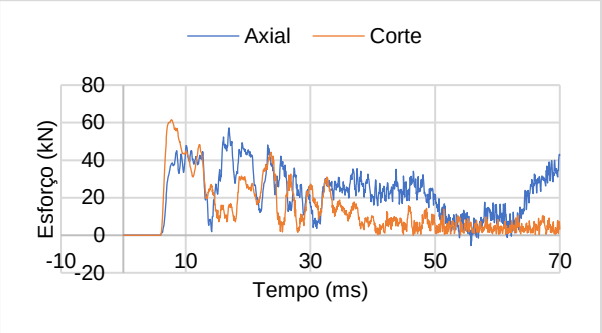

Ilustration 7 – Axial and shear forces on top *Bolt 1*.

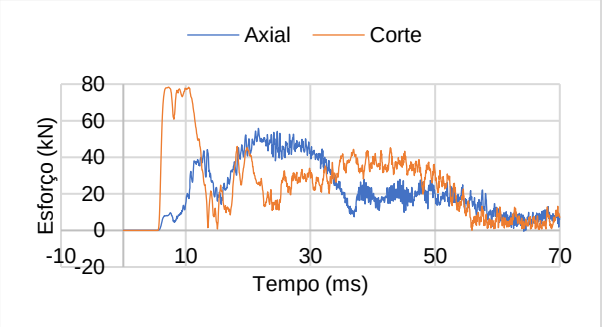

Ilustration 83 - Axial and shear forces on medium height *Bolt 1*.

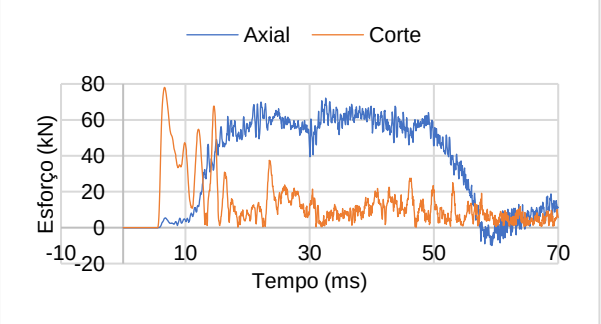

Ilustration 9 – Axial and shear forces on bottom *Bolt 1*.

Next, another indicator that can be presented are the areas in which the steel is S275 and that suffer plastic deformation. It is possible to know the zones in which steel S275 is plasticized, assigning a change of colors to the software when a yield extension of 0.275/210=0.001310 is reached. Next, these results are presented in the

form of views obtained from the software (**Illustration 10, Ilustration 11** and **Ilustration 12**).

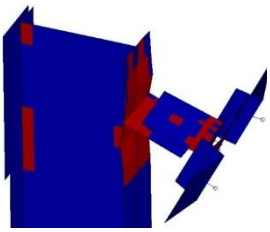

Ilustration 10 – Plastification of S275 on top connection.

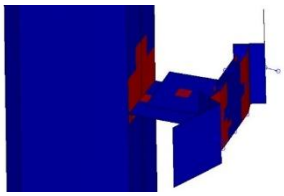

Ilustration 11 – Plastification of S275 on middle connection.

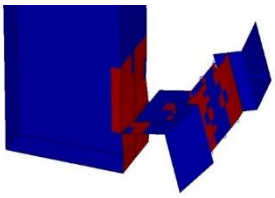

Ilustration 12 – Plastification of S275 on bottom connection.

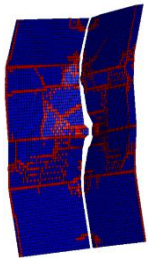

Illustration 13 – Break zones on glass.

The same procedure can be done to know in which areas the S460 steel elements, perpendicular sheets, plasticize. However, it is not a relevant result, to be presented here, because it was found that the perpendicular plates never plasticize. A relevant result, is to perform this procedure to know in which zones the glass reaches the rupture, assigning a change of colors to the software when it reaches an extension of yield of 0.09845/70 = 0.001406. The remote view shows this result in **Illustration 13**.

5.4. Results interpretation

This section is for the analysis and interpretation of the results obtained in the previous section. Through the first set of results, those referring to axial and cutting forces in Bolts 1, it is possible to remove several ideas and notice some aspects that will be described below.

There are two bolts that receive more energy than one other. We are talking about differences in efforts in the order of 20 kN. The half-height and base bolts are clearly subject to greater efforts than the top of the facade bolt, strictly 80kN and 60kN, respectively, at the maximum moment of shear ≈7.5ms). This means that the shock wave is reflected on the ground just before reaching the structure, creating the Mach stem, which further powers the explosion.

These elements (bolts) essentially work at shear, in almost all the analysis. However, it is important to note that the bolt of the base connection works most of the time also axially. This is due to the fact that, when the glass gives way and starts to bend, it pulls the lower fixing of the glass panels. The biggest displacement in the glass is, therefore, between the inferior fixation and the one of half-height. Next, it is important to highlight the areas where the structure plasticizes and to make some comments about it. The areas of the profile in which the steel plasticizes are: the three areas where the fixation elements of the glass are connected; and the upper area of the fixed support. As they plasticize these zones, they also plasticize *Plate 1* in the place where they are connected to the IPE. In the area surrounding *Bolts 1* the yield strength of S275 steel is reached and in the lateral areas of *Plate 4* where the perpendicular plates are connected, this happens again. Regarding the glass element, this forms an interesting breaking pattern and only continued in one piece due to the fact that the PVB film, although it has also reached the yield in some places of the panels, keeps the fragments united to itself, maintaining the integrity (not structural) of the glass.

5.5. Energy dissipator study

In reference to the subtitle of the present work, an attempt was made to develop a solution for the protection of glass facades against explosions. In this case this solution is a dissipator manufactured in metamaterial PETg and with hexagonal cell structure, as presented in **Illustration 14.** The constitutive law of the dissipator tested, with the established dimensions of 100x100x50 mm^3, is expressed in **Illustration 15**.

Illustration 14 – PETg honeycomb dissipator.

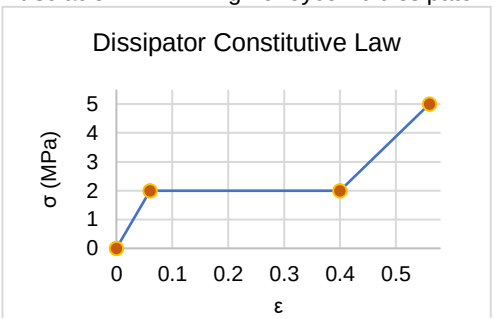

Illustration 15 – Dissipator constitutive law.

However, this was not the constitutive law modelled. With the continuity of running models, it was verified that it would be necessary to increase the resistance of the dissipator, because for the dynamic action of explosion, its characteristics did not even prove sufficient. Then it was proceeded to increase of 20% the stiffness of the dissipator, which in practice means to increase the thickness of the walls of the metamaterial alveoli, being with a yield stress of 2,4 MPa (instead of 2 MPa) and with an ultimate stress of 6 MPa (instead of 5 MPa).

In the next paragraphs, the results

obtained from the models with dissipator will be analyzed. Regarding the efforts on the screws the following results were obtained (**Illustration 16,**

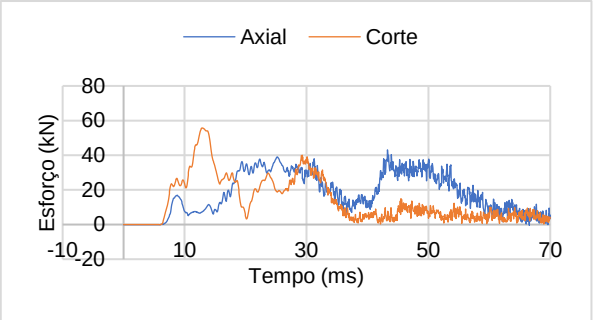

Ilustration 16 – Axial and shear on top *Bolt 1*, with dissipator.

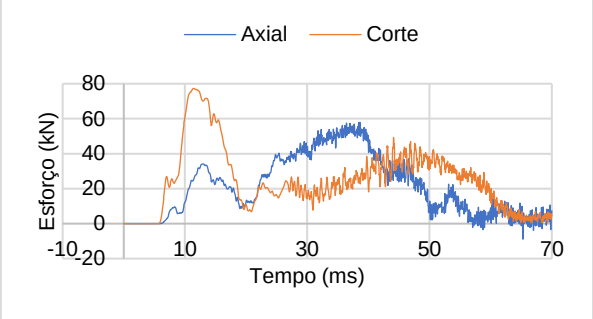

Ilustration 17 – Axial and shear on middle *Bolt 1*, with dissipator.

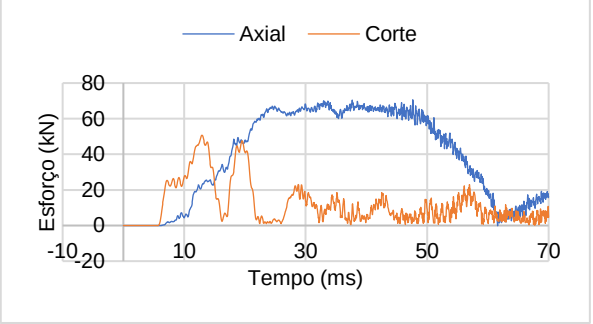

Ilustration 18 – Axial and shear on bottom *Bolt 1*, with dissipator.

In the first instance, it is possible to say that the efforts that reach *Bolts 1* of this model are smaller compared to the reference model. Similarly to the reference model, for *Bolt 1* of the top fixing there was an improvement of about 5 kN; for the bolt of the half-height fixation, there was practically no difference in terms of maximum shear force; and for the bolt of the facade base fixation, this did have a significant difference, about 30 kN. It is also possible to state that, by observing the 6 bolt graphs, the response of the structure with integrated dissipator is a more cushioned response, and not a response with great energy dissipation, there are fewer variations, less "ups and downs". This happens at least up to about 25 ms of analysis, which corresponds to the moment when the dissipator undergoes its maximum compression and consequent densification. This densification induces a more rigid response and from that moment on the model starts to have a more similar response to the reference model. It is also important to mention that the maximum shear moment on the bolts takes place about 12.5 ms of analysis; and that as soon as the shock wave reaches the structure, a shear force peak as in the reference model no longer occurs.

Next, the areas where the S275 steel of the structure plasticizes will be analyzed (**Illustration 19, Illustration 20** and **Illustration 21**):

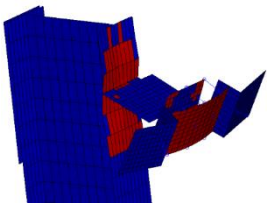

Ilustration 19 – Plastification of S275 on top connection, with dissipator.

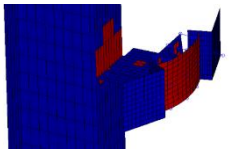

Ilustration 20 – Plastification of S275 on middle connection, with dissipator.

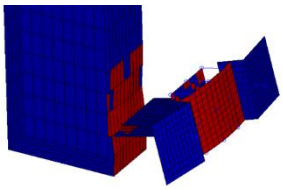

Ilustration 21 – Plastification of S275 on bottom connection, with dissipator.

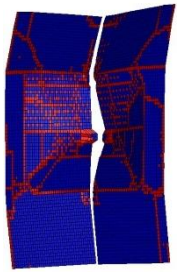

Ilustration 22 – Break zones on glass, with dissipator.

In this model, it only plasticizes the surrounding area of the half height screw. This may be due to the dissipator that makes the fixing structure respond more uniformly to the action and better redistributes the stresses. The plasticized areas of the IPE profile are also practically the same as the reference model. In the dissipator model, it happens that *Plate 4* suffers a large curvature and fully plasticizes, and not only the lateral edges, as in the reference model.

The glass of the model with dissipator, presents another but similar pattern of rupture, suffering greater curvature between the fixation of top and half height, than that presented in the reference model. This may be due to the fact that the fixing system with the dissipator is less rigid and does not make vertical displacements so difficult (**Illustration 22**).

VI. Experimental tests program

In view of future developments within this dissertation, the setups for prescribing tests without dissipator and with dissipator are explained below. It is intended that the experimental tests will be done on a real scale and therefore real controlled explosions will be tested, and not inside a shock tube. Both in the reference tests and in the dissipator tests, the load will be 10 meters away

from the outer face of the glass and at a height of 1.5 meters (half the height of the glass façade).
This facade is supported by 3 IPE200 profiles 3 meters high that support two 3 meter high and 2 meter wide laminated glass panels.

As far as dissipator tests are concerned, it is necessary to insert it, as already mentioned, between the two vertical sheets of the secondary support structure. Obviously, some of the values previously mentioned can be adjusted in order to consider an explosion with a different reduced distance parameter:

- Mass of TNT charge = X kilograms of TNT;
- Height of the charge above the ground = Y meters;
- Horizontal distance of the charge = Z meters.

Of course, some instrumentation equipment will be needed in order to characterize the tests. They may be the following or similar:

- Deformation sensors;
- Pressure sensors;
- High speed cameras;
- Accelerometers.

VII. Final considerations

7.1. Summary and main conclusions

A correct analysis of any protection system of a structure is crucial to consider three elements: the protection system, the structural elements and the actions.

In the present dissertation several aspects concerning glass and its behaviour as a structural element were investigated. Glass can be a structural element inserted in VEC and VEA facades. In the exterior stapled glass façades, the possibilities of fixing solutions are immense or almost infinite. As in this work, if a fixation system geometry was invented, a new system can appear every day. The chances are many and the freedom is great.

In order for the glass panels not to present so much curvature, they would have to have better mechanical properties, have greater thickness or different support conditions.

In all models there was a clear formation of the *Mach stem*, for the characteristics given to the explosion, because the facade receives more load from half-height to the base. Therefore, there is, of course, reflection in the ground plane and later potentiation of the shock wave and the incident impulse itself.

By the analysis of the results, the dissipator did not have such a dissipative impact, as was expected to be obtained at the beginning of the development of this dissertation. It is certain that it is able to slightly cushion the load that passes to the structure, however it does not absorb what is necessary to be implemented in infrastructures that need it.

The models, which generated the results present in Chapter V, took about 2 hours and 20 minutes to fully run. Despite being three-dimensional models resulting from elements with 2D geometry, it is possible to conclude, in the first instance, that this program generates, as a rule, very slow and heavy analyses. However, it is considered a software of multiple applications in which it is possible to specify the smallest characteristic.

More than 80 models were run in total and each one took 2 hours on average.

7.2. Future work

Finally, it is possible to say that, although the behavior of the developed protection solution is not the best, in general it has been able to accomplish what was intended. However, during the development of the present dissertation some ideas have emerged that are worth giving importance in the future:

- Evidently, experimental results were lacking to compare with the computational models developed, and therefore it is considered important to do so in the future;
- Study of the behavior of glazed facades during the negative phase of explosions and ways to protect them or mitigate impacts;
- Development of dissipators in metamaterials with other geometries and different framing in load-bearing structures of glass facades. It would be interesting to consider glass supported all along its edge in elements of this type or supported occasionally, but in fixing systems with other characteristics;
- Use of metamaterials in further studies underway in our country, as they constitute a new piece of knowledge that deserves to be studied and understood by more Portuguese people;
- Use of metamaterials in the protection of structures against seismic action.

References

[1] «Human Rights , Terrorism and Counter-terrorism - Fact Sheet No. 32», New York, 2008.

[2] University of Maryland, *Global Terrorism Database Codebook*, n. junho. 2017.

[3] S. and T. Department of Homeland Security, *Reference Manual to Mitigate Potential Terrorist Attacks Against Buildings*, n. outubro. 2011.

[4] L. Valarinho, F. Branco, G. Chiumiento, e J. Correia, «Instabilidade lateral por flexão-torção de vigas em vidro estrutural. Estudo experimental e analítico.», *5as Jornadas Port. Eng. Estruturas*, pp. 1–16, 2014.

[5] J. M. C. P. de N. Sanches, «Análise e Dimensionamento de Sistemas Estruturais de Vidro», Universidade Técnica de Lisboa, 2013.

[6] H. S. Norville e E. J. Conrath, «Simplified Design Procedure for Blast Resistant Glazing», *ResarchGate*, n. junho, pp. 18–21, 2001.

[7] T. Ngo, P. Mendis, A. Gupta, e J. Ramsay, «Blast Loading and Blast Effects on Structures - An Overview», *Eletronic J. Struct. Eng.*, n. janeiro, pp. 76–91, 2007.

[8] «Unified Facilities Criteria (UFC) - Structures To Resist the Effects of Accidental Explosions», 2008.

[9] E. Yandzio e M. Gough, «Protection of Buildings against Explosions», *Steel Constr. Inst.*, p. 120, 2011.

[10] G. Kinney e K. Graham, *Explosive shocks in air*, 2ª. Nova Iorque: Springer Science + Business Media, LLC, 1985.

[11] V. Karlos e G. Solomos, «Calculation of blast loads for application to structural components», 2013.

[12] V. Karlos, G. Solomos, e M. Larcher, «Analysis of the blast wave decay coefficient using the Kingery–Bulmash data», *Int. J. Prot. Struct.*, vol. 7, n. 3, pp. 409–429, 2016.

[13] H. Draganić e V. Sigmund, «Blast Loading on Structures», *Technical Gazette 19*, vol. 19, n. 3, Ozijek, pp. 643–652, 2012.

[14] M. Shaheen, «Numerical Modelling of Blast Loads effects on a Reinforced Concrete Structure Using LS-DYNA Software», Islamic University Of Gaza, 2015.

[15] M. Förch, «Analysis of Glass Panels Subjected to Blast Load», HafenCity Universitat Hamburg, Hamburg, 2019.

[16] S. B. Janney, «Blast Resistant Design of Steel Structures», University of Tennessee, Knoxville, 2007.

[17] G. de J. Gomes, «Reutilização de edifícios correntes para fins operacionais - Blast Assessment», 2016.

[18] J. Pinto, «Comportamento de Estruturas de Aço sob a Ação de Explosões - Conceção de dissipadores de energia», Academia Militar, 2018.

[19] C. E. Needham, *Blast Waves*. Albuquerque, 2010.

[20] S. M. M. Pereira, «Estudo do Comportamento Estrutural de Fachadas em Vidro», Universidade Nova de Lisboa, 2012.

[21] C. S. M. P. Costa, «Controlo da Qualidade de Fachadas em Vidro - Fachadas-Cortina e Fachadas em Vidro Exterior Agrafado», Universidade de Lisboa, 2018.

[22] H. D. Hidallana-Gamage, D. P. Thambiratnam, e N. J. Perera, «Computational analysis of laminated glass panels under blast loads: a comparison of two dimensional and three dimensional modelling approaches», *Int. J. Eng. Sci.*, vol. 2, n. 8, pp. 69–79, 2013.

[23] M. Lopo e P. Coutinho, «Mitigação de impactos com estruturas auxéticas impressas em 3-D .», 2019.

[24] M. Parratt, «Behaviour of Multi-Layered Laminated Glass Under Blast Loading», University of Toronto, 2016.

[25] Livermore Software Technology Corporation (LSTC), Ed., *LS-DYNA ® Theory Manual*. Califórnia, 2015.

[26] «LS-DYNA, Um solver para múltiplas aplicações», *Distrim*. [Em linha]. Disponível em: https://www.distrim.pt/ls-dyna/. [Acedido: 04-Set-2020].